Available online at www.sciencedirect.com
ScienceDirect
Ceramics International 36 (2010) 1283–1288
CERAMICS INTERNATIONAL
www.elsevier.com/locate/ceramint

The effect of the wet-milling process on sintering temperature and the amount of additive of SiAlON ceramics

Onur Eser [a], Semra Kurama [b,*]

[a] Graduate Department of Advanced Technologies, Anadolu University, Eskisehir, Turkey
[b] Anadolu University, Department of Materials Science and Engineering, Eskisehir 26555, Turkey

Received 3 September 2009; received in revised form 20 November 2009; accepted 27 December 2009
Available online 29 January 2010

Abstract

In this study, nano-sized SiAlON powders were produced by wet milling at elevated speeds as a top-to-bottom process. Before the milling process, different milling times and mediums were performed for the determination of the most efficient milling system. The milled powders were characterized by BET and X-ray diffraction (XRD) measurements and the results were compared to standard samples. The standard powders were produced using a conventional process (the ball to powder ratio was 1:1.5, at 300 rpm, for 1.5 h) having a few hundred nanometer particle size. The nano powders were milled using a wet-milling process in an optimum medium so that the particle size was decreased down to ≈70 nm. The samples, produced from the nano powders, were densified at 150 °C lower degrees than the sintering temperature of samples which were produced by a conventional method (185 nm). However, the phase transformation of $\alpha \rightarrow \beta$-SiAlON was also observed related to the amount of additives. This transformation affected the mechanical properties of the SiAlON ceramic. The results were discussed using the relationship between density, phase composition, microstructure and mechanical properties.

Keywords: A. Milling; D. SiAlON; C. Mechanical Properties; A. Sintering

1. Introduction

A special focus on SiAlON ceramics is related to their excellent mechanical properties (hardness, fracture toughness, strength), good corrosion and thermal shock resistance. Silicon nitride (Si_3N_4) based ceramics, such as SiAlON's, are made of powders and all these properties depend on the quality of the starting powders. Sintering of Si_3N_4 ceramics is very difficult because of the strong covalent bonding between the Si and N atoms. Therefore, there should be pressure assist and/or sufficient amount of sintering additive to obtain fully dense SiAlON ceramics. Usually, metal and rare earth oxides are used as sintering additives which promote densification through liquid phase sintering. During sintering, the oxide additives react with silica on the surface of the Si_3N_4 particles to form a vitreous flux at sintering temperature assisting mass transportation during densification. However, the intergranular soft glassy or crystalline phase that remains in the dense body is important for high temperature properties [1]. Additionally, the particle size of starting powders and the sintering temperature play an essential role on both the sintering behavior and the cost of processing. So, many investigations have been focused on the preparation of nano-sized SiAlON powders to decrease the sintering temperature and increase the mechanical properties [2–4].

There are certain methods for the preparation of nano-sized SiAlON powders such as plasma-chemical [2] and laser synthesis [3], sol–gel [4] and, as a top-to-bottom process, high-energy mechanical milling [5]. Zalite and co-workers [2] obtained fully dense ceramics from plasma-chemical synthesized SiAlON nano powders at relatively low temperatures (1500–1600 °C) with good mechanical properties. Although this method promises very low particle sizes (∼40 nm) it would increase the cost of the initial powder [6]. Xu et al. [5] show that particle size of SiAlON starting powders could be decreased to nano-size by using a high-energy mechanical milling process which includes dry milling. However, such dry milling systems lead to the wearing of milling equipment and contaminants in the milled powder [6].

---

* Corresponding author. Tel.: +90 222 321 3550x6372; fax: +90 222 323 9501.
E-mail address: skurama@anadolu.edu.tr (S. Kurama).

0272-8842/$36.00 © 2010 Elsevier Ltd and Techna Group S.r.l. All rights reserved.
doi:10.1016/j.ceramint.2009.12.025

In a conventional method, wet milling is a process used to obtain a homogeneous powder mixture. However, the efficiency of the milling could be increased and become a top-to-bottom process by changing critical variables. Agglomerates formed during the milling could exhibit a critical effect on the milling performance because the energy produced by vial and balls is used to break up agglomerates. Thus, in an agglomerate-free system, energy will be transferred to the powder to decrease particle size. There are few studies [7–10] investigating well-dispersed suspension systems for SiAlON ceramics but these did not include any comparison between solvent and dispersant types. In this study, SiAlON powders milled in different solvent mediums (toluene, methyl ethyl ketone, and ethanol) with different kinds of dispersants (oleic acid, poly ethylene glicol, sodium tripolyphosphate) and sedimentation tests were performed. According to the sedimentation test results the most dispersed suspension was selected. This system was used as a milling medium in further steps of this study.

The aim of the present study is to investigate the most effective wet-milling system for the production of nano SiAlON powder. This work was carried out in two parts. In the first part, the influence of the milling system on the particle size of the starting powders and the sintering temperatures was examined. In the second part, the effect of particle size on the amount of additive was investigated.

2. Experimental procedure

2.1. Preparation of suspensions

In the general formula of α-SiAlON described as $M_xSi_{12-(m+n)}Al_{(m+n)}O_nN_{16-n}$, the composition doped with Y_2O_3 was prepared from a starting powder mixture of Si_3N_4 (UBE-10, containing 1.6 wt.% oxygen), AlN (Tokuyama, containing 1 wt.% oxygen), Al_2O_3 (99.99 wt.%, Sumitomo AES IIC) and Y_2O_3 (99.99 wt.% HC Starck). The starting composition is given in Table 1.

The weighed powders were milled by planetary ball milling (Pulverisette 6 Fritsch, Germany) with the Si_3N_4 balls for 2 h in different solvent compositions (toluene, methyl ethyl ketone, ethanol, Table 2). The solvent compositions were determined according to literature studies [7–12]. The sedimentation method was used for determination of an adequate dispersion in order to use ball milling energy to decrease the particle size of the starting powders. The suspensions were transferred to sealed cylindrical glass tubes and the sediment heights were measured every 0.5 h for 3 h. After the determination of the most dispersed solvent composition, three kinds of dispersants (*oleic acid* (Codex, Carlo Erba), *polyethyleneglicol* (PEG, M.W.: 8000, Aldrich) and *sodium tripolyphosphate* (STPP, Esan, Turkey)) were added to the mixture at different ratios (0.5–3 wt.%) to perform sedimentation tests.

Table 1
Overall composition of the starting materials (wt.%).

Sample code	Materials (wt.%)			
	Si_3N_4	AlN	Al_2O_3	Y_2O_3
C	76.22	13.45	3.83	6.50

Table 2
Solvent compositions of milling medium.

Solution code	Solvent ratio (vol.%)		
	Ethanol	Toluene	Methyl ethyl ketone
7M/3E	30	–	70
6M/4E	40	–	60
5T/2M/3E	30	50	20
3T/4M/3E	30	30	40
6T/4E	40	60	–
10E	100	–	–
4T/3M/3E	30	40	30
2T/4M/4E	40	20	40
2T/8E	80	20	–
5T/5E	50	50	–
4T/6E	60	40	–
3T/7E	70	30	–

The cavity in the closed packed system of the Si_3N_4 balls was measured and filled with SiAlON suspension which had a 10 vol.% solid load for high efficiency. The milling studies for this mixture were carried out at 450 rpm for 10, 20, 30 and 40 h. The samples are called *SX*. *X* represents the milling time of the powder. The standard powders mixture was prepared using a conventional method (the ball to powder ratio was 1:1.5, at 300 rpm, for 1.5 h) denoted as *C*. The contamination caused by the milling balls and/or vial was calculated by weighting them before and after the milling process.

The mixed powder was uniaxially pressed at 1.96 MPa into pellets of 15 mm diameter and 4–5 mm thickness. After uniaxial pressing they were pressed at 250 MPa by cold isostatic press (CIP) to increase their green density. Sintering was carried out in a gas pressure sintering furnace (in FPW 180/250-2-220-100SP, FCT) in a nitrogen atmosphere (2.2 MPa) at different temperatures (1790–1940 °C) for 2 h. The particle size distribution and specific surface areas of the milled powders were determined using scanning electron microscopy (Zeiss, Supra 50 VP) and the BET nitrogen method. The equivalent grain size (D_{BET}) is calculated according to the following equation, based on the BET specific surface area:

$$D_{BET} = \frac{6}{\delta x S} \tag{1}$$

In this equation, δ represents the theoretic density (g/cm^3) of the powder [13]. The density of the starting mixture (δ) was calculated as 2.95 g/cm^3. The crystalline phases of the powders and the sintered samples were identified using an X-ray diffractometer (Rigaku Rint 2000, Tokyo, Japan) with Cu Kα radiation (λ = 1.540 Å) from 5° to 60° with a scanning speed of 2°/min. The Archimedes method was used to determine the bulk density of the sintered samples. Additionally, the microstructural characterization of the sintered samples was investigated by scanning electron microscopy (Zeiss, Evo 50). For mechanical test analyses, the hardness was measured using a Vickers diamond indenter on a polished surface with a 10 kg load. The K_{IC} values were calculated using the following formula [14,15]:

$$K_{IC}[\mathrm{MPa}^{1/2}] = k\left(\frac{E}{H}\right)^{1/2} F \times c^{-3/2} \times 0.0316 \qquad (2)$$

where E = Young's Modulus (320 GPa), H = hardness (GPa), F = load (N), c = crack length (μm), k = dimensionless constant 0.016 ± 0.004.

$$H_V(\mathrm{GPa}) = \frac{0.47 \times P}{a^2} \qquad (3)$$

where P = applied force (10 kg), a = half of the length of the diagonal indentation.

3. Results and discussion

3.1. Sedimentation tests

The stability of SiAlON suspensions was evaluated by the settling of powder (sedimentation height) for different types of solvent at 10 vol.% solid content. In Fig. 1, the effect of the solvent types and their ratio on the sedimentation height of the suspension is given. It can be seen that a binary solvent system of ethanol (E) and toluene (T) at a volume ratio of 70:30 has the highest sedimentation height. This result indicates that this is the most dispersed solvent composition. Therefore, this composition was selected for further investigation of the most efficient dispersant. The effect of the dispersant in selected solvent composition was investigated by the addition of oleic acid, STPP (*sodium tripolyphosphate*) and PEG (*polyethyleneglicol*, M.W. 8000). The maximum sedimentation height that could be obtained was 115.6 mm by the addition of 1 wt.% PEG. However, this sedimentation height is lower than that of the 70E/30T system in which it is about 120 mm (Fig. 2). As a consequence, the binary solvent system of 70E/30T without any addition of dispersant shows the most dispersed behavior and is used as a milling medium for milling studies.

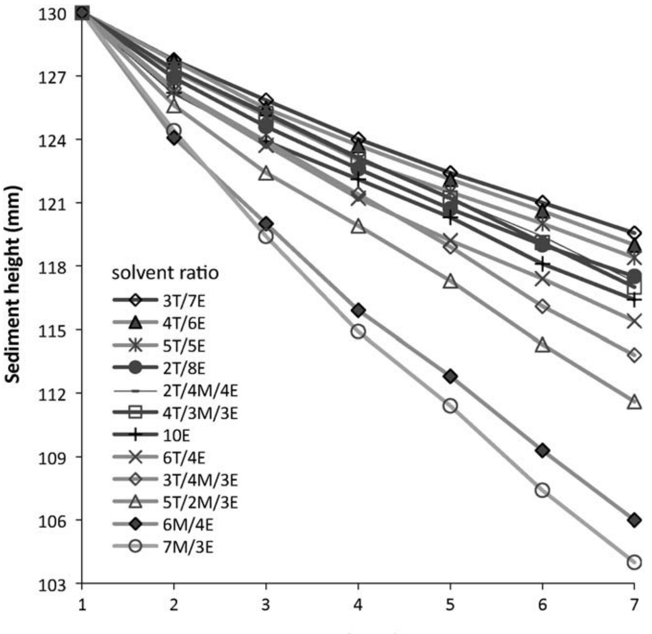

Fig. 1. Sedimentation height as a function of time for different kinds of solvents (E: ethanol; T: toluene; M: methyl ethyl ketone).

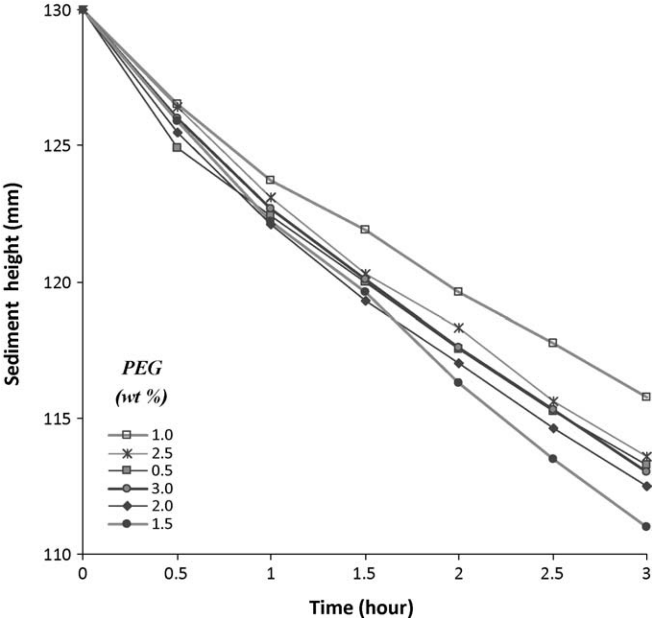

Fig. 2. Effect of amount of PEG on sedimentation height.

3.2. Milling and powder characterization

The milling time effect on the powders was characterized by X-ray diffraction (XRD) analysis and the results are given in Fig. 3. The peaks of the powders started to widen by increasing the milling time which indicates a reduced particle size. While an AlN peak was observed in the *C* powder, it disappeared by increasing the milling time. This result can be explained by increasing the amount of the amorphous phase. As indicated the study of Sopicka-Lizer et al. [6] the AlN particles have little resistance to deformation during the milling process. The result supports the reason for the disappearance of the AlN peaks in this study, as seen in the XRD analysis, by increasing the milling time.

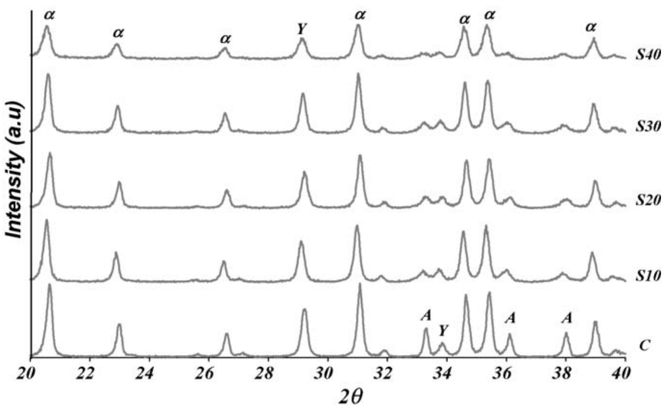

Fig. 3. XRD patterns of milled powders (α: Si_3N_4; A: AlN; Y: Y_2O_3).

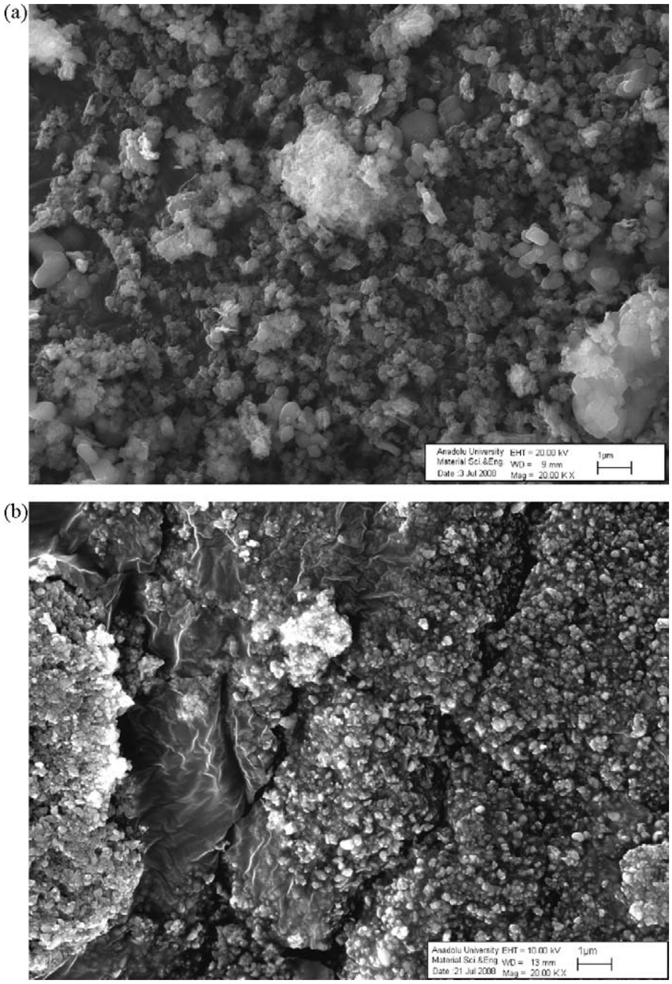

Fig. 4. SEM micrographs of milled powders (a) *C*; (b) *S40*.

Table 3
Specific surface area (*S*) and equivalent grain size (D_{BET}) of the milled powders.

Sample	*C*	*S10*	*S20*	*S30*	*S40*
S (m^2/g)	11	14.1	17.6	20.7	27.5
D_{BET} (nm)	185	144	115	98	74

Fig. 4 gives the SEM micrographs of the *C* and *S40* samples. It is very difficult to calculate and compare the average particle size of the powders using SEM micrographs, but it gives an idea of particle size distribution. The *S40* has homogeneous particle size, about 100 nm, while the powder *C* is more heterogeneous than the *S40*, and its particle size changes from 100 nm to 1 μm.

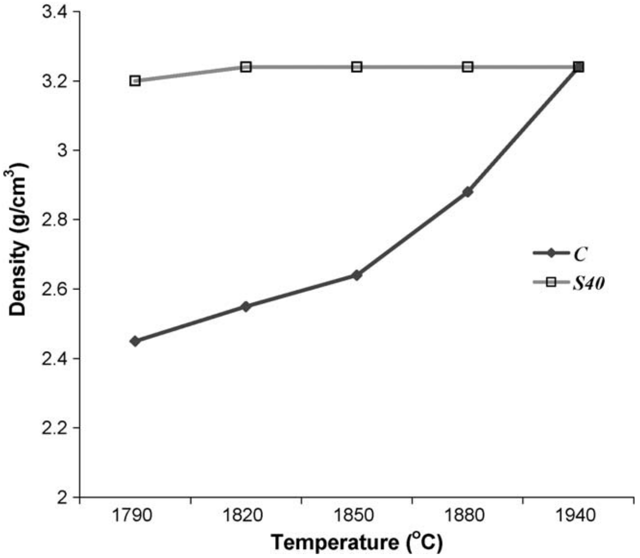

Fig. 5. Changing density of samples, produced by conventional (*C*) and high-energy milling (*SX*) methods, by decreasing sintering temperature.

For a realistic measurement, the BET method was used and the D_{BET} of the powders was calculated (Table 3). The results show that the *S40* powder has the highest specific surface area (27.5 m^2/g) and the finest particle size (74 nm). A 30% increase in surface area between the *S30* (20.7 m^2/g) and the *S40* (27.5 m^2/g) powders was observed while this value is about 20% for the *S10–S20* and the *S20–S30* powders. The difference in increase of the surface of the powders can be explained by the storage of elastic energy produced by the balls and its release during the 40 h milling process.

3.3. Sintering and mechanical properties

According to the BET analysis results, the *S40* powder has the highest surface area and the lowest powder size. Therefore, the *S40* sample was selected for use in future sintering process and analysis parts of this study. Additionally, the *C* powder also sintered as a standard to compare with the results of the *S40*. The sintering was carried out in a gas pressure sintering furnace at different temperatures for 2 h. The changing density of the samples (*C* and *S40*) related with temperature is given in Fig. 5. It can be observed that fully densified *C* samples could be only obtained at 1940 °C. When the temperature was decreased from 1940 to 1790 °C, the density was decreased to ∼2.45 g/cm^3. Even though the *S40* was doped with a lower amount of Y_2O_3 (5.5 wt.%) than the *C* samples (doped with 6.5 wt.%

Table 4
Relationship between density, mechanical properties and phase composition of samples at different temperatures.

Sample code	Sintering temperature (°C)	Density (g/cm^3)	Hardness (HV10)	Fracture toughness (MPa m$^{1/2}$)	Phase ratios (wt.%)
C	1940	3.24	18.0	6.35	100α
S40	1880	3.24	17.40	6.00	55α:45β
S40	1850	3.24	17.80	6.20	50α:50β
S40	1820	3.24	16.35	6.90	20α:80β
S40	1790	3.20	16.10	6.95	10α:90β

Table 5
Relationship between density, mechanical properties and phase composition of samples doped with different amount of Y_2O_3.

Sample, wt.% Y_2O_3	Sintering temperature (°C)	Density (g/cm^3)	Hardness (HV10)	Fracture toughness (MPa m$^{1/2}$)	Phase ratios (wt.%)
C-6.5	1940	3.24	18.00	6.35	100α
S40-5.5	1850	3.24	17.80	6.20	50α:50β
S40-3.5	1850	3.22	16.30	6.75	15α:85β
S40-2.5	1850	3.20	16.10	6.90	11α:89β

Y_2O_3) it showed an almost full density up to 1790 °C. According to the XRD results, by decreasing the sintering temperature a $\alpha \rightarrow \beta$ phase transformation has occurred (Table 4). This transformation can be explained by hydrolysis of AlN during the milling process and this resulted in an increase of oxygen content in composition. Therefore, the composition may shift from a stability region of α-SiAlON to β-SiAlON. Also, the stability of β-SiAlON at lower temperatures ensures the formation of the β-phase. Due to the high amount of the α/β-SiAlON ratio and the low sintering temperature, the *S40* sample, sintered at 1850 °C, was selected for future investigation in this study.

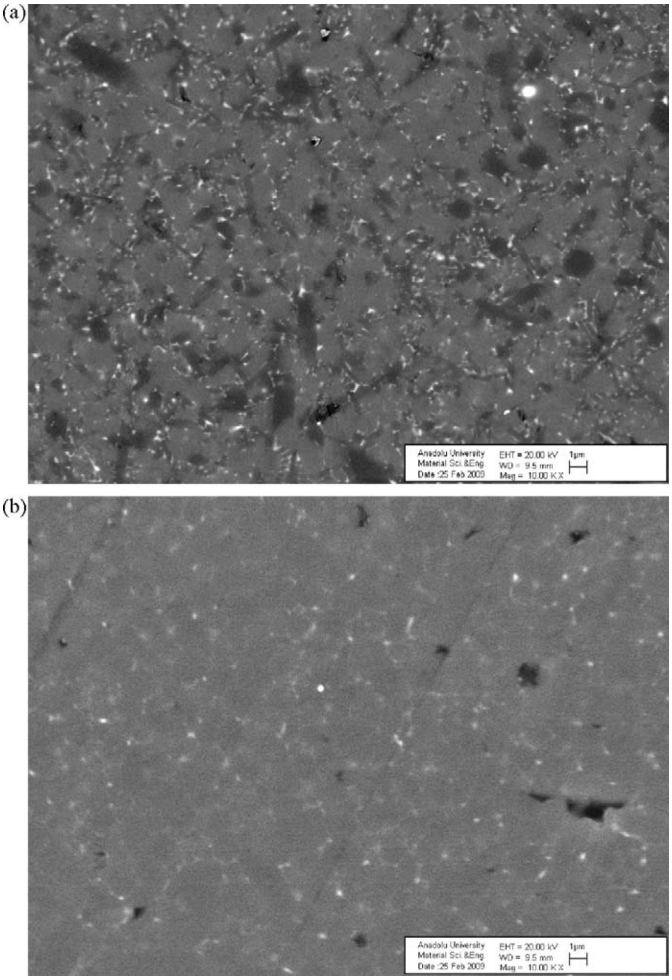

Fig. 6. SEM micrographs of (a) *S40-5.5* sample sintered at 1850 °C; (b) *C-6.5* sample sintered at 1940 °C.

In the second part of this study, the amount of the sintering additive was decreased related with the sintering temperature. The results are given in Table 5 and it can be seen that the mechanical properties were also changed. Even though the density of the samples was not much affected by decreasing the amount of Y_2O_3 up to 2.5 wt.%, it was noted that decreasing the amount of Y_2O_3 significantly affected the mechanical properties. The changes in the mechanical properties can be explained by the $\alpha \rightarrow \beta$ SiAlON phase transformation. As seen in the literature, the α-SiAlON has an important effect on hardness whereas the β-SiAlON has a positive effect on the toughness of samples [16]. Comparison of the *C-6.5* and the *S40-5.5* samples clearly indicates that it is possible to obtain fully dense SiAlON ceramics with the same mechanical properties at a 90 °C lower sintering temperature than that of the *C-6.5* with a lower amount of additives using nano powders. The microstructural comparison of the *C-6.5* and the *S40-5.5* samples is given in Fig. 6.

4. Conclusion

This study shows that high-energy milling in a wet medium system is an effective method for the production of nano-sized SiAlON starting powders. By using this method the highest BET specific surface area was obtained (27.5 m^2/g) after milling for 40 h and this value indicates an equivalent particle size of 74 nm. Therefore, samples which were produced from nano powders could be densified at 150 °C degrees lower than the sintering temperature of samples which were produced by a conventional method at 1940 °C. During the sintering of samples related with the sintering temperature, the amount of additives and the milling medium (ethanol), the $\alpha \rightarrow \beta$-SiAlON phase transformation was also observed. This transformation can be explained by the hydrolysis of the AlN powder during the milling process and a shifting starting composition from the α-SiAlON phase region to β-SiAlON related with an increasing oxygen amount in the composition. Additionally, the amount of additive could also be reduced by decreasing the powder size of the starting composition in the *S40* sample without decreasing density. However, decreasing the amount of the additive from 5.5 to 3.5 wt.% or lowering the amount of Y_2O_3 has significantly affected the mechanical properties of the samples. As a consequence, by using nano powders, fully dense SiAlON ceramics were produced at a lower sintering temperature of 90 °C than that of the *C-6.5* sample with the same mechanical properties (hardness and fracture toughness) and with a lower amount of additives.

References

[1] K. Chihara, D. Hiratsuka, J. Tatami, F. Wakai, K. Komeya, High-temperature deformation of α-SiAlON nanoceramics without additives, Scripta Materialia 56 (2007) 871–874.

[2] F. Bulic, I. Zalite, N. Zhilinska, Comparison of plasma-chemical synthesised SiAlON nano-powder and conventional prepared SiAlON powder, Journal of the European Ceramic Society 24 (2004) 3303–3306.

[3] R. Dez, F. Ténégal, C. Reynaud, M. Mayne, X. Armand, N. Herlin-Boime, Laser synthesis of silicon carbonitride nanopowders; structure and thermal stability, Journal of the European Ceramic Society 22 (2002) 2969–2979.

[4] Q. Li, C. Zhang, K. Komeya, J. Tatami, T. Meguro, L. Gao, Nano powders of β-SiAlON carbothermally produced via a sol–gel process, Journal of Materials Science Letters 22 (2003) 885–887.

[5] X. Xu, T. Nishimura, N. Hirosaki, R. Xie, Y. Yamamoto, H. Tanaka, Fabrication of β-SiAlON nanoceramics by high-energy mechanical milling and spark plasma sintering, Nanotechnology 16 (2005) 1569–1573.

[6] M. Sopicka-Lizer, M. Tancula, T. Wlodek, K. Rodak, M. Huller, V. Kochnev, E. Fokina, K. MacKenzie, The effect of mechanical activation on the properties of β-SiAlON precursors, Journal of the European Ceramic Society 28 (2008) 279–288.

[7] X. Xu, M. Oliveira, J.M.F. Ferreira, Effect of solvent composition on dispersing ability of reaction sialon suspensions, Journal of Colloid and Interface Science 259 (2003) 391–397.

[8] P. Reis, J.P. Davima, X. Xu, J.M.F. Ferreira, Tribological behaviour of colloidally processed SiAlON ceramics sliding against steel under dry conditions, Tribology Letters 18 (3) (2005) 295–301.

[9] Z.J. Lü, X. Ai, J. Zhao, Preparation of agglomerate-free starting powders for TiC-reinforced β-SiAlON nanocomposites, Materials Science Forum 471–472 (2004) 282–286.

[10] N.C. Acikbas, E. Suvaci, H. Mandal, Fabrication of functionally graded SiAlON ceramics by tape casting, Journal of American Ceramics Society 89 (10) (2006) 3255–3257.

[11] H.L. Liu, C.Z. Huang, J. Wang, J. Sun, Microstructure and mechanical properties of two kinds of Al_2O_3/SiC nanocomposites, Materials Science Forum 471–472 (2004) 243–247.

[12] J. Hwang, B.I. Lee, D. Kim, S. Wi, Effects of solvent composition on the rheological behavior of $CaZrO_3$-based dielectrics and glass suspensions, Colloids and Surfaces A: Physicochemistry and Engineering Aspects 289 (2006) 60–64.

[13] Z. Wang, R. Hui, N. Bogdanovic, Z. Tang, S. Yick, Y. Xie, I. Yaroslavski, A. Burgess, R. Maric, D. Ghosh, Plasma spray synthesis of ultra-fine YSZ powders, Journal of Power Sources 170 (2007) 145–149.

[14] K.E. Amin, Thoughness, hardness and wear, Engineering Materials Handbook Ceramics and Glasses, vol. 4, ASM International, 1991, pp. 601.

[15] A.G. Evans, E.A. Charles, Fracture toughness determinations by indentation, Journal of American Ceramics Society 59 (1976) 371.

[16] C. Zhang, K. Komeya, J. Tatami, T. Meguro, Inhomogeneous grain growth and elongation of Dy-α SiAlON ceramics at temperatures above 1800 °C, Journal of the European Ceramic Society 20 (2000) 939–944.